Renewable Energy 114 (2017) 934–944

Contents lists available at ScienceDirect

Renewable Energy

journal homepage: www.elsevier.com/locate/renene

Comparative study of the thermal performance of four different shell-and-tube heat exchangers used as latent heat thermal energy storage systems

Jaume Gasia [a], Jan Diriken [b, c], Malcolm Bourke [c], Johan Van Bael [b, d], Luisa F. Cabeza [a, *]

[a] GREA Innovació Concurrent, INSPIRES Research Centre, Universitat de Lleida, Pere de Cabrera s/n, 25001, Lleida, Spain
[b] Flemish Institute for Technological Research (VITO), Boeretang 200, BE-2400, Mol, Belgium
[c] Glen Dimplex Renewables (GDC), Church Road, Portadown, Co Armagh, BT63 5HU, UK
[d] Energyville (Joint Venture of VITO NV and KU Leuven), Thor Park 8300, BE-3600, Genk, Belgium

ARTICLE INFO

Article history:
Received 6 November 2016
Received in revised form
22 April 2017
Accepted 28 July 2017
Available online 28 July 2017

Keywords:
Thermal energy storage
Phase change material
Shell-and-tube
Heat exchanger
Key performance indicators

ABSTRACT

In this paper, the influence of the addition of fins and the use of two different heat transfer fluids (water and a commercial silicone) have been experimentally tested and compared in four latent heat thermal energy storage systems, based on the shell-and-tube heat exchanger concept, using paraffin RT58 as phase change material. Three European institutions were involved under the framework of the MERITS project. A common approach (temperature and power profiles), and five different key performance indicators have been defined and used for the comparison: energy charged, average power, 5-min peak power, peak power to energy ratio, and time. For the same heat transfer fluid, results showed that finned designs (4.7–9.4 times more heat transfer surface) showed an improvement of up to 40%. On the contrary, for the same design, water (which has a specific heat 3 times higher and a thermal conductivity 4.9 times higher than silicone Syltherm 800), yielded results up to 44% higher.

1. Introduction

The energy-related emission of greenhouse gases and the increasingly common difficulty of energy supply are economic, environmental and social problems that need to be faced. Hence, the implementation of eco-friendly techniques that reverse current trends in energy supply and demand becomes crucial. Among them, renewable energy sources play an important role since they can support these energy security and climate change goals. However, the large areas of land required, a high dependence on the weather and the mismatch between the energy demand and supply are three main drawbacks that hinder large scale successful implementation of renewable energy technologies. In order to overcome these constraints, storage technologies, especially thermal energy storage (TES), have become an important and necessary component [1].

Three different TES systems can be identified: sensible, latent and thermochemical. In sensible heat storage, the thermal energy is stored as a result of a change in the storage material temperature. In latent heat storage, the thermal energy is stored as a result of a phase change process of the storage material. Finally, in thermochemical storage the thermal energy is stored in the form of a reversible chemical reaction between two substances. Latent heat thermal energy storage (LHTES) has drawn attention in the scientific community due to high storage densities and narrow operating temperatures [1]. Phase change materials (PCM) have been widely used for LHTES applications for a variety of purposes and several studies have been done to review the materials, heat transfer and applications of TES systems incorporating PCM in different applications [2,3].

Mehling and Cabeza [1] described the criteria in designing complete heat storage systems for both sensible and latent TES purposes. Table 1 shows the four main LHTES systems based on the storage density and the loading and unloading power curve. In a direct contact system the heat transfer fluid (HTF) is in contact with the PCM, which eliminates the additional thermal resistance of the intermediate container material. Direct systems have high storage densities because up to 90% of their volume is PCM. They usually have medium to high power because of direct contact between the HTF and PCM and the forced convection which exists in the storage

* Corresponding author.
E-mail address: lcabeza@diei.udl.cat (L.F. Cabeza).

http://dx.doi.org/10.1016/j.renene.2017.07.114

Table 1
Thermal energy storage types: Working principles and general performance. Adapted from Mehling and Cabeza [1].

Storage type	Working principle	General performance
Direct contact	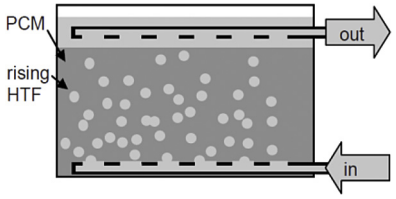	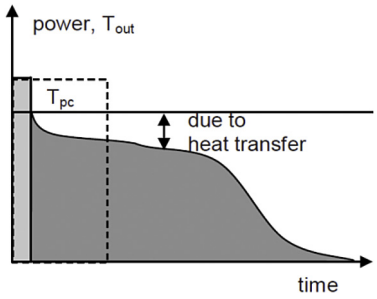
Modular	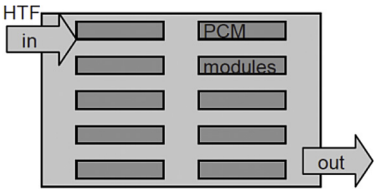	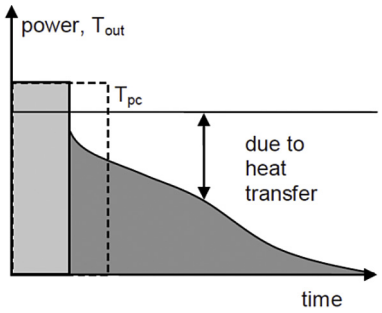
Slurry	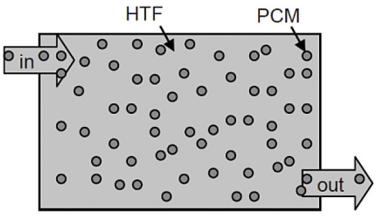	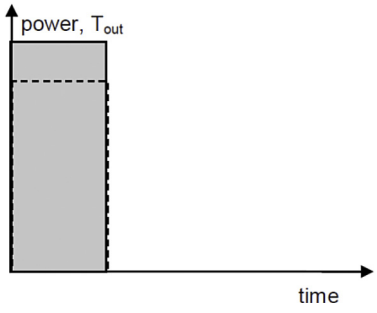
Heat exchanger	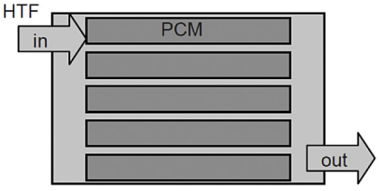	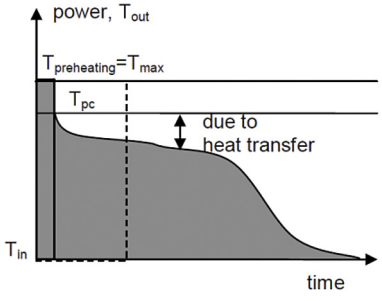

system. In a modular system the PCM is macro-encapsulated in modules and placed in a storage tank. This system has a medium energy density due to the following factors: a combination of sensible heat stored by the HTF and latent heat stored by the PCM; a decrease in the power absorbed/released from initially high magnitudes due to preheated HTF within the storage tank, to subsequently lower values due to thermal resistance of the macrocapsules. In a slurry system the PCM is microencapsulated and mixed with the HTF, ensuring a fluid-like behaviour of the mixture. This system has higher storage density and power than the pure HTF because the microcapsules effectively increase the energy density. Finally, in a heat exchanger system, the PCM is placed in a storage vessel and the HTF flows through a network of pipes placed within the vessel. This system has high storage density because up to 95% of the volume is PCM [1]. A decrease in the power absorbed/released from an initial very high value also occurs, with a decrease from a high difference between the inlet and outlet HTF temperatures, to a medium-low value.

The heat exchanger system evaluated in the present study was based on the shell-and-tube concept. This concept consists of a storage vessel, where the PCM is located, and a determined number of tubes placed within the vessel through which the HTF flows causing the heat exchange between both elements. Shell-and-tube heat exchangers have been widely studied by several authors under different boundary conditions during charging and discharging processes (HTF mass flow rates, HTF inlet temperatures, heat transfer enhancement techniques, and type of PCM). These studies mainly analysed the shell-and-tube configuration with only one

tube but some approaches using many tubes have also been studied.

Among the research work which studied the simple tube configuration, the most extended analysis was the numerical evaluation of the thermal behaviour under various HTF operation conditions and geometric parameters [4–7]. It was determined that these conditions and parameters depended on the desired heat transfer rate and process time, but faster processes were obtained with higher temperatures and mass flow rates. Akgun et al. [8] experimentally studied the charging and discharging processes under different inlet temperatures and mass flow rates in a tilted vertical shell and tube heat exchanger using paraffin P1 as PCM and water as HTF. Results showed a decrease in the melting time with higher values of mass flow rate and inlet temperature. Medrano et al. [9] experimentally evaluated the charging and discharging processes of five commercial heat exchangers using paraffin RT35 as PCM and water as HTF. Three of them were based on the shell-and-tube concept, and the other two were based on the compact plate and frame concept. Results showed that under the same working conditions, the compact heat exchanger showed highest average thermal power, as a result of the high ratio of heat transfer to external volume. The thermal performance of shell-and-tube heat exchangers using various tubes (also referred as multitubes) has been studied by different researchers. Ismail and Abugderah [10] numerically analysed the importance of Reynolds and Stefan numbers in vertical multitube configurations, avoiding the use of empirical correlations. Moreover, they noted that the most important parameters in these systems are the outer radius and system length. Hendra et al. [11] and Agyenim et al. [12] experimentally and numerically studied the multitube concept using Mikro and Erythritol as PCM respectively. They observed the high influence of convection heat transfer in the liquid fraction of PCM.

Low thermal conductivity values of current cost-effective PCM hinder the optimum thermal performance of LHTES systems. Hence, the implementation of heat transfer enhancement techniques has been studied in order to overcome this drawback. Among them, the addition of fins has been found to be very attractive. This technique increases the heat transfer surface by using highly conductive material, resulting in an increase in the heat transfer rate. Several authors have numerically and experimentally studied the influence of adding fins to the thermal performance of LHTES systems [13–16]. Results showed higher heat transfer rates and faster processes when compared to the same systems without fins. Moreover, they studied how the modification of their geometrical parameters (number of fins, fin dimensions, fin spacing, and fin material) enhanced the heat transfer. It was observed that better results were obtained for the systems with higher numbers of fins, when the space between fins was reduced, when bigger fins were used or when fins made of materials having higher thermal conductivity were used.

The aim of this paper is to experimentally evaluate four different heat exchanger systems based on the shell-and-tube concept under the framework of the MERITS project (ENER/FP7/295983) in order to quantify and compare the influence of the addition of fins and the use of different HTF on the thermal performance. All experiments have been performed using paraffin RT58 as PCM and under the same boundary conditions and methodology.

2. Materials and methodology

2.1. Materials

2.1.1. Phase change material

In the present study, the selected PCM was paraffin RT58. The main reasons for its selection were the good properties of paraffin, and the melting temperature range of RT58 specifically, which was suitable for domestic hot water (DHW) and industrial waste heat (IWH) recovery purposes. The choice to use this PCM was shared by the three institutions as all were part of a collaborative study through the European research project MERITS (ENER/FP7/295983).

The thermophysical properties of this material according to the manufacturer are summarized in Table 2. Previous studies have shown the suitability of paraffin RT58 as PCM [17]. Samples of the RT58 used in the investigated set-ups were also analysed using differential scanning calorimeter (DSC) analysis (see Section 3.1).

2.1.2. Heat transfer fluids

Two different HTFs were selected to evaluate their influence on the thermal behaviour of the LHTES system. The first HTF was water, a fluid which has been used for thermal carriage purposes for ages and whose thermal characteristics are widely known. The second HTF was Syltherm 800, a silicone fluid whose molecular base consisted of dimethyl polysiloxane $(C_2H_6OSi)_n$ [19]. Fig. 1 shows a comparison of the thermophysical properties of the two HTFs used in the present experimentation.

2.2. Experimental set-ups

Figs. 2–4, show a general overview of the experimental setups used by the University of Lleida, VITO and Glen Dimplex, respectively.

The high temperature pilot plant used at the University of Lleida was an integration of three main systems: a heating system, a cooling system, and a storage system. The heating system consisted of a 24 kW_e electrical heater capable of heating the HTF up to 380 °C. The 20 kW_{th} air-HTF heat exchanger of the cooling system was used to reduce the temperature of the HTF. Finally, the storage system was a set of two identical shell-and-tube tanks only one of them incorporated 196 squared fins. The different systems were connected with a pipe system and insulated with rock wool. Silicone fluid Syltherm-800 was used as HTF and was circulated with a 4 kW pump up to a volumetric flow of 3 m^3/h. Valves were manually operated to determine the flow direction of the HTF. Measuring equipment was placed around the installation in order to control and acquire information and data related to the HTF flow rate, HTF temperatures, and HTF pressures at a time interval of 30 s.

The VITO thermo-technical laboratory was designed to deliver thermal powers up to 400 kW in a working temperature range between 6 °C and 88 °C. The selected HTF was water, which was stored in three storage vessels at high, medium and low temperature levels. The desired temperature was obtained by mixing the water from these vessels before delivering it to the different experimental set-ups. The laboratory was equipped with a gas-fired boiler for hot water preparation, and a dry-cooler to obtain low fluid temperatures. The different experimental set-ups were hydraulically separated from the primary loop for safety purposes. All valves and pumps were operated by a NI Labview interface which controlled specific loading and unloading sequences. Data was logged in a SQL database with a minimal sampling time of 200 ms. For the present experiments, a sampling time of 1 min was used. The PCM storage vessel was also equipped with a cross-flow mechanism which allowed rapid inversion of the flow direction through the vessel, and a by-pass section which could be used to preheat or cool the HTF before starting the HTF circulation.

The test facility of Glen Dimplex consisted of a 500 L buffer store coupled to a 37.6 kW industrial chiller and 12 kW air source heat pump. The HTF was water. This configuration allowed preconditioning of the HTF to temperatures between 6 °C and 70 °C as required, and was capable of delivering a constant temperature HTF flow to the PCM store for the duration of each test. During the

Table 2
Thermophysical properties of RT58 according to the manufacturer [18].

Properties	Values	Units
Melting area	53–59	[°C]
Congealing area	59–53	[°C]
Heat storage capacity ±7,5%	160	[kJ/kg]
(combination of latent and sensible heat in a temperature range of 50 °C to 65 °C)	48	[Wh/kg]
Specific heat capacity	2	[kJ/(kg·K)]
Density solid (at 15 °C)	0.88	[kg/L]
Density liquid (at 80 °C)	0.77	[kg/L]
Heat conductivity (both phases)	0.2	[W/(m·K)]
Volume expansion	12.5	[%]
Flash point	>200	[°C]
Max. operation temperature	80	[°C]

charging process, pre-heated HTF supplied energy to the PCM from the buffer store. During the discharging process, pre-cooled HTF absorbed energy from the PCM and subsequently flowed to the chiller for re-cooling, simulating a heating demand. The control/regulating valves were manually operated and the heat pump and chiller were controlled by independent control units. The HTF pumps were operated using NI Labview software, which also recorded flow rates and temperatures at 2 s intervals from appropriately placed instrumentation in the test rig. These included flow and temperature sensors in the HTF, and 31 temperature sensors in the PCM.

2.3. Storage systems

The storage systems evaluated in the present study (Figs. 5 and 6) were based on the shell-and-tube heat exchanger concept, and consisted of a storage vessel with a tube bundle embedded inside. The PCM was placed in the space between the storage vessel walls and the tube bundle, through which the HTF circulated. In this experimentation, the storage vessels had a rectangular prism shape and the tubes were distributed in square pitch and bended in a U-shape in order to have both the HTF inlet and outlet distribution manifolds at the same side of the storage tank.

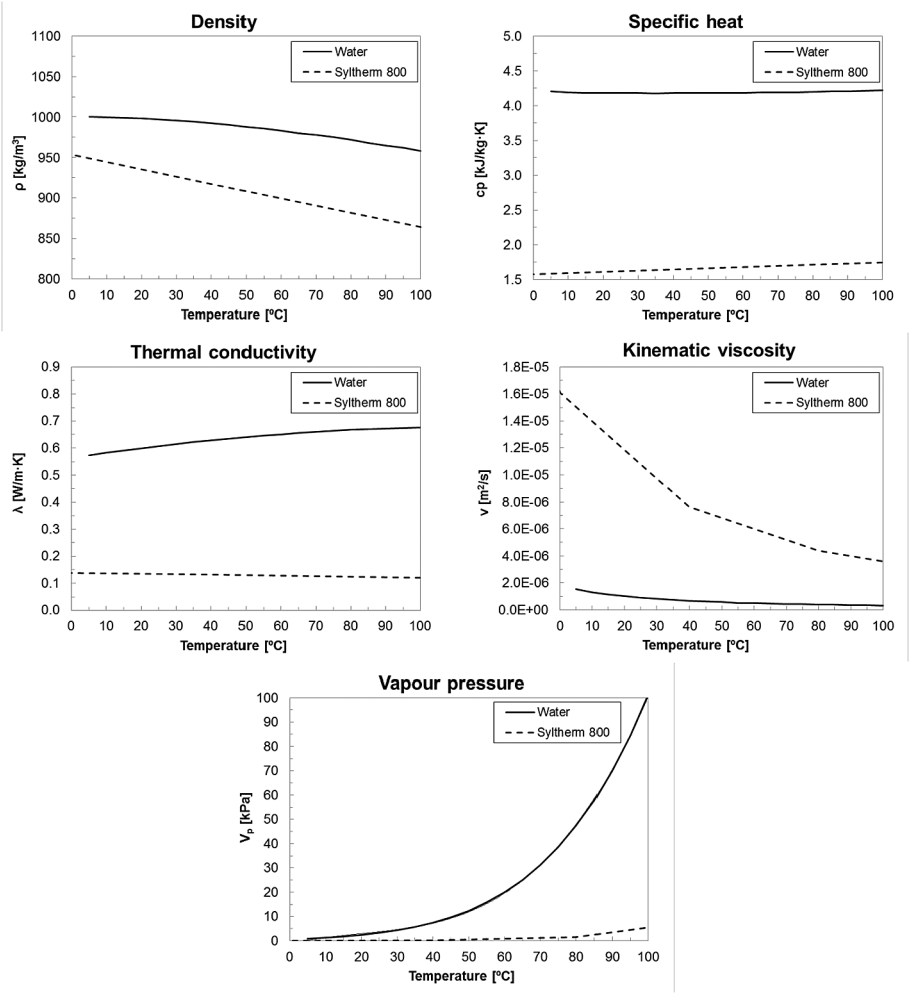

Fig. 1. Comparison of the thermophysical properties of the two HTFs evaluated.

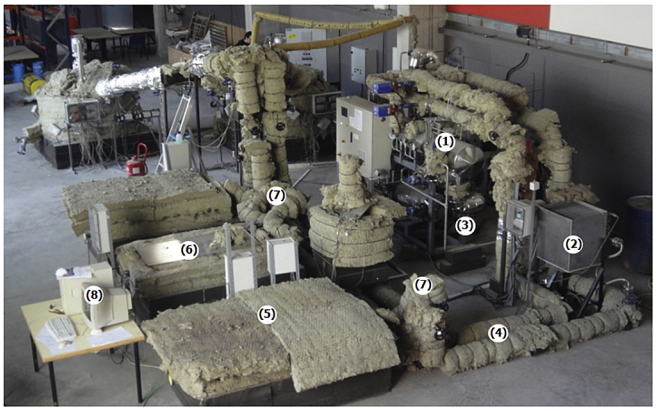

Fig. 2. Overview of the experimental setup of the University of Lleida: (1) Electrical heater; (2) Air-HTF heat exchanger; (3) HTF recirculation pump; (4) HTF distribution piping; (5) Storage tank 1: without fins; (6) Storage tank 2: with fins; (7) HTF distribution valves; (8) Acquisition and recording system.

Fig. 3. Overview of the experimental setup of VITO: (1) High-temperature storage vessel; (2) Medium-temperature storage vessel; (3) Low-temperature storage vessel; (4) Supply mixing valve 1 (high and medium temperature); (5) Supply mixing valve 2 (low temperature); (6) Primary-secondary side heat exchanger; (7) Supply/return station to flex setups; (8) Connection to storage vessel.

The main design characteristics of the storage tanks evaluated are presented in Table 3. Notice that some parameters of the four storage systems were different to allow the researchers to perform and discuss a wider range of experiments. The first parameter was the distribution and geometry of the tubes in the tube bundle. While the tube bundle of both storage tanks of the University of Lleida (Fig. 5) and the tank of Glen Dimplex (Fig. 6b) consisted of 49 tubes distributed in squared pitch and a similar average length, the VITO design (Fig. 6a) differed as there were eight tubes which crossed the vessel length multiple times (they travelled down the vessel in eight stages). Hence, they had an average length almost three times greater than the previous tanks. The second parameter was the number of fins and their distribution along the tube bundles. The storage tank with fins of the University of Lleida (Fig. 5b) had 196 squared fins which were in contact with the 49 tubes, and the storage tank of VITO (Fig. 6a) had eight sets of 130 rectangular fins. Each fin was in contact with four pipes twice. Finally, the third and last parameter was the HTF type used. At the University of Lleida the selected HTF was the silicon fluid Sylltherm 800, while at the facilities of VITO and Glen Dimplex the selected HTF was water.

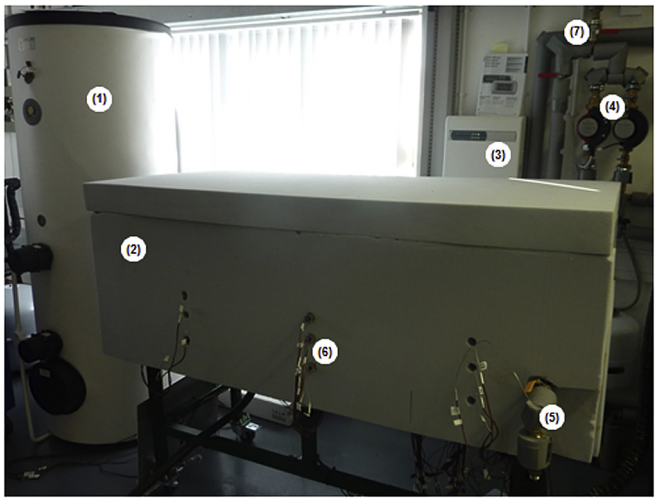

Fig. 4. Overview of the experimental setup of Glen Dimplex: (1) 500 L Buffer Store; (2) PCM tank with foam insulation; (3) Heat pump controller; (4) HTF circulation pumps; (5) Connection to PCM store; (6) Thermocouple entry points to PCM tank; (7) Manual ball valves.

In order to carry out an accurate analysis of the thermal behaviour of the PCM during the experimentation, several temperature sensors were installed in each tank as Fig. 7 shows. At both storage tanks of the University of Lleida, 19 Pt-100 temperature sensors (3 wire, class B, accuracy ± 0.1 °C at 80 °C), with an accuracy of ±0.1 °C, were located within the tube bundle. They were distributed in three different heights, at 31 mm, 126 mm, and 190 mm from the bottom of the tank and at nine different distances (at 38 mm, 78 mm, 118 mm, 532 mm, 612 mm, 692 mm, 1227 mm, and 1273 mm from the side of the distribution manifolds). Two additional Pt-100 temperature sensors, with an accuracy of ±0.1 °C, were used to monitor the HTF temperature at the inlet and outlet of the tank. At the storage tank of VITO, nine Pt-100 (3 wire, class B, accuracy ± 0.55 °C at 50 °C) temperature sensors were used to monitor the PCM temperature. The measuring points were located at three different depths (100 mm, 200 mm, and 300 mm) at three points along the central axis of the vessel, in between the fins. These three locations were at 10 cm, 20 cm, and 30 cm from the top of the storage tank. Also the temperature of the HTF before and after the vessel was monitored by PT-100 (3 wire, class 1/10 DIN) along with the HTF flow rate. Finally, the temperature of the PCM in the storage tank of Glen Dimplex was measured using 31 T type thermocouples, with an accuracy of ± 1.0 °C. The thermocouples were situated within the tube bundles at three heights (31 mm, 126 mm, and 190 mm) from the bottom of the tank and were inserted at 6 different depths (35 mm, 75 mm, 114 mm, 150 mm, 194 mm, and 250 mm from the sides of the tank) in order to obtain a broad spectrum of temperature readings. Same type thermocouples were placed in the HTF at the connections to the PCM tank to record the HTF temperature. A Grundfos VFS 2–40 L/min flowmeter (accuracy ± 1.5% FS) recorded the HTF flowrate.

2.4. Methodology

Before performing the experimentation at the three laboratories, a DSC analysis was carried out to determine the consistency in the phase-change temperature and enthalpy of the PCM samples. The authors used a DSC-822e commercialized by Mettler Toledo which was available at the University of Lleida. These samples were sealed in an aluminium crucible under an inert atmosphere of N_2 and were subjected to a dynamic process between 50 °C and 65 °C

(a) (b)

Fig. 5. Overview of the thermal energy storage tanks used at the University of Lleida: (a) without fins; (b) with fins.

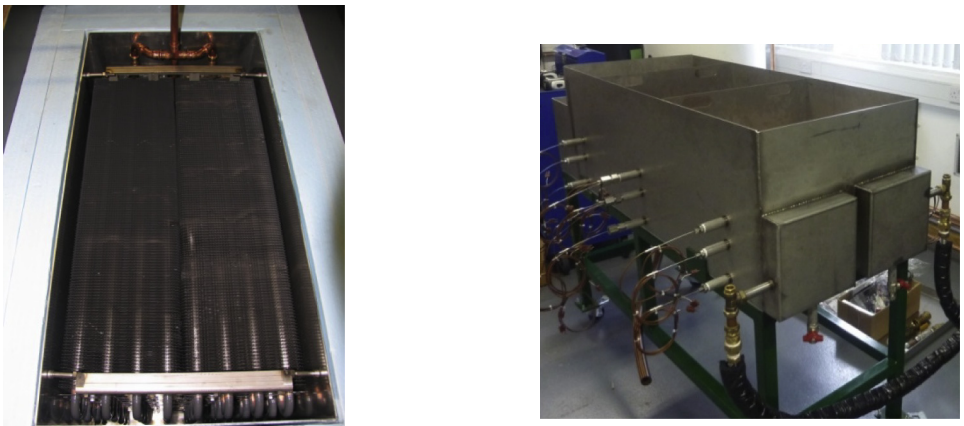

(a) (b)

Fig. 6. Overview of the thermal energy storage tank used at (a) VITO and (b) Glen Dimplex.

Table 3
Characteristics of the storage systems.

Parameter	University of Lleida (without fins)	University of Lleida (with fins)	VITO	Glen Dimplex
Material of the tank	Stainless steel 304 L	Stainless steel 304 L	Aluminium	Stainless steel 304 L
Tank width [mm]	527.5	527.5	420	540
Tank depth [mm]	273	273	495	440
Tank length [mm]	1273	1273	865	1250
Number of pipes [–]	49	49	8	49
Type of pipe surface	Smooth	Smooth	Smooth	Smooth
HTF pipes average length [mm]	2485	2485	6800	2385
Inner diameter of the pipes [mm]	13.2	13.2	13.2	13.6
Thickness of the pipes [mm]	2	2	1.5	0.7
Number of fins [–]	–	196	8 × 130	–
Dimension of fins [mm]	–	250 × 250	110 × 200	–
Thickness of fins [mm]	–	0.5	0.5	–
Distance between fins [mm]	–	10	5.2	–
Heat transfer surface [m^2]	6.55	31.05	46.60	5.45
Tank vessel volume [m^3]	0.183	0.183	0.180	0.297
PCM volume [m^3]	0.145	0.141	0.136	0.134
PCM mass [kg]	107.5	106	121.7	118.4
Packing factor [–]	0.837	0.804	0.901	0.651
Insulation	240 mm of rockwool	240 mm of rockwool	60 mm of styrofoam	100 mm of basotech foam

at heating and cooling rates of 0.5 °C/min.

The experiments carried out consisted of charging processes within the temperature range of 48–68 °C and at a HTF mass flow rate of 500 kg/h. This mass flow rate was chosen based on the operational limitations of the three facilities. A stabilization period was required before starting the charging process to obtain a uniform and homogeneous initial state of the PCM. The homogeneous initial state was achieved by recirculating the HTF through the storage tank at the initial temperature of charging (48 °C). When the PCM temperature was stable, the HTF temperature was

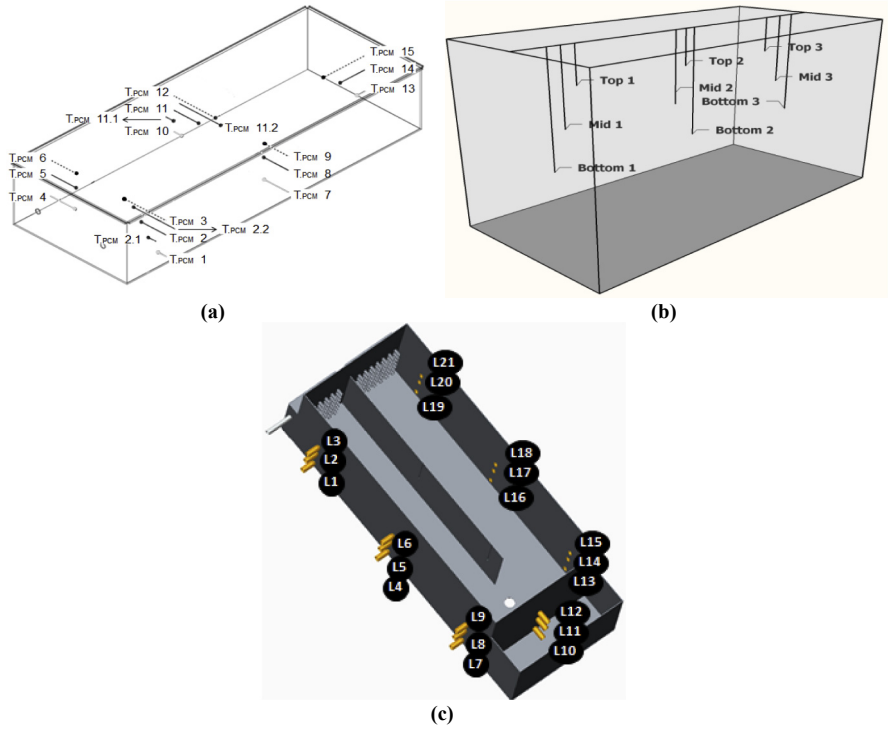

Fig. 7. Location of the temperature sensors within the storage tanks: (a) University of Lleida (both tanks); (b) VITO; (c) Glen Dimplex.

increased to the charging temperature (68 °C), and the process started. The inlet HTF temperature for the entire duration of the charging process was 68 °C ± 2 °C. The charging process was concluded after 6 h of circulating the HTF.

3. Results and discussion

3.1. Material analysis

Table 4 and Fig. 8 show a comparison between the DSC results from the RT58 samples used by the three institutions. Notice that all the samples have similar values with slight differences caused by the inherent DSC error, the mass of the samples and their technical grade. Thus, the DSC results allowed the three institutions to perform a direct comparison of the pilot plant results. Moreover, the enthalpy values obtained with the DSC analysis were also different from the values presented by the manufacturer (Table 2). Reasons for this may be as discussed above, and additionally the use of different techniques and methodology to determine the values.

3.2. Storage systems analysis

In the following section the results of the measurements are discussed. The effect of the HTF used in the different configurations as well and the effect of the addition of fins were evaluated by fixing one parameter. The results are shown in Fig. 9 (temperature profiles) and Fig. 10 (normalised power profiles). Notice that in the temperature profiles shown in Fig. 10, only the most representative sensors were selected to be shown for a better visualization of the temperature evolution over time. In the case of the VITO system, only very small temperature differences were observed between all sensors at the same height. Therefore the average values of the sensors at same height are shown. In Fig. 10, normalised and absolute power profiles are shown. The normalisation was done for each storage system individually by normalising the charging power curve to the maximal instantaneous charging power of that system. In this way the time behaviour of the charging power curve could be compared for all systems, as well as with the theoretical power profile shown in Table 1.

Table 5 shows a summary of the results obtained from different key performance indicators (KPI) during the experimentation performed. First, the total energy charged during the total measurement (6 h). Second, the average power during the charging process. Third, the 5-min peak power, which was the maximum value of the averaged power at time intervals of 5 min. This value is presented to remove the effect of the HTF fluctuations. Fourth, the peak power to energy ratio, which provides a comparison between the 5-min peak power in relation to the energetic size of the energy store. The higher the number, the more efficient the heat exchanger was in

Table 4
Summary of the DSC results from the RT58 samples used by the three institutions.

Institution	Mass of the sample [mg]	Melting enthalpy [kJ/kg]	Solidification enthalpy [kJ/kg]	Melting Temperature [°C]	Solidification Temperature [°C]
University of Lleida	12.77	125	154	58	58
VITO	11.52	152	148	58	58
Glen Dimplex	25.72	147	139	58	57

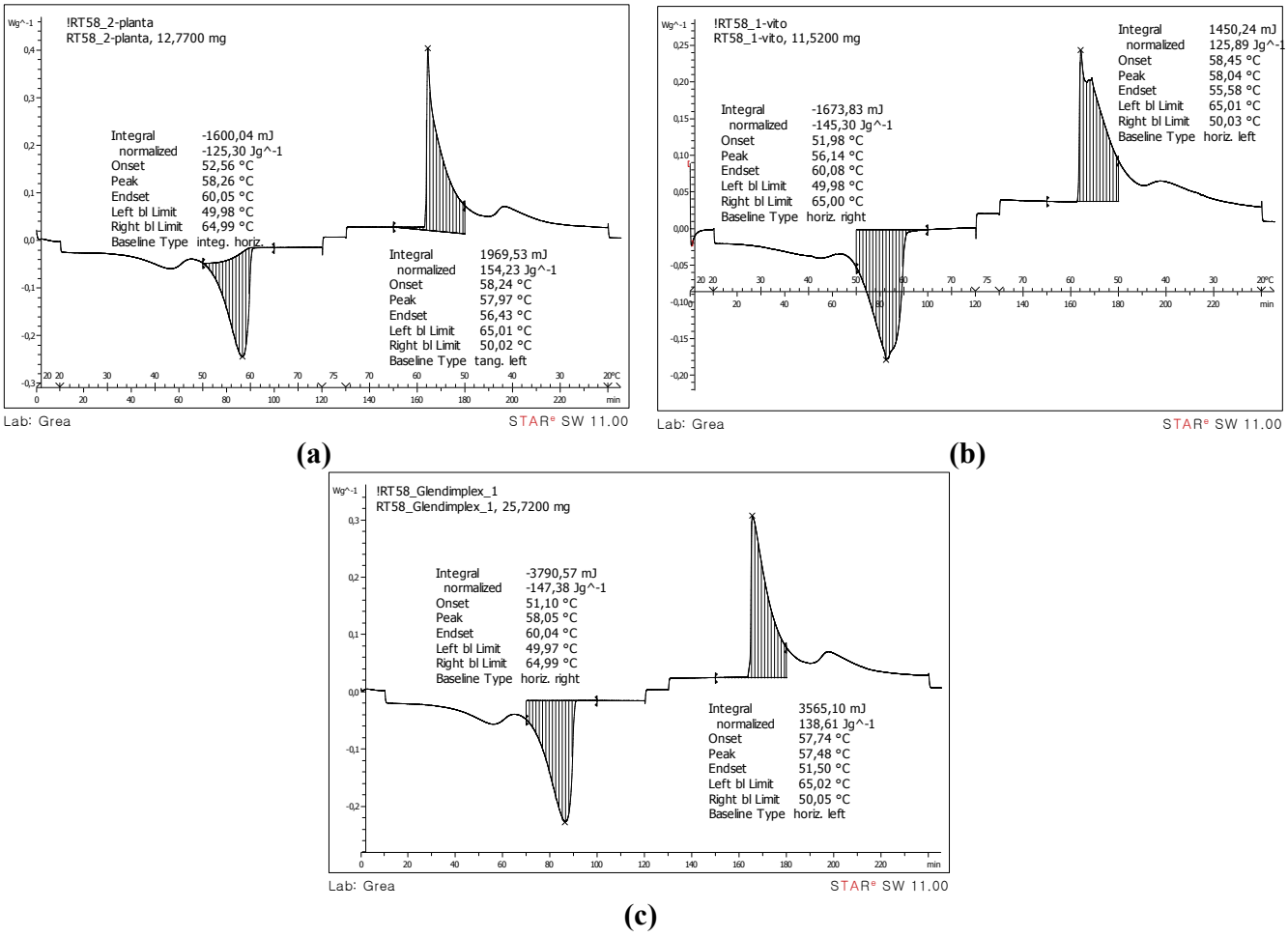

Fig. 8. DSC results of the RT58 samples: (a) University of Lleida; (b) VITO; (c) Glen Dimplex.

delivering peak power from the store. Since the PCM content (and hence the energy content of the storage units) was nearly equal in all cases considered here, the 5-min peak power can be used as well for comparison. Finally, the time needed, in minutes, to fully charge the PCM and reach the stop condition.

3.3. *Influence of the addition of fins*

The effect of the addition of fins on the thermal performance of the LHTES systems has been evaluated by comparing the storage systems which used the same HTF. Note that all results can be directly compared since the quantity of PCM of both systems was comparable (Table 3).

Both the VITO and Glen Dimplex designs used water as HTF. However, the VITO design was equipped with fins, while the Glen Dimplex design was not. Results show that the finned design was 24% faster than the non-finned design. Furthermore, the finned design could sustain an elevated power output for a prolonged period of time compared to the non-finned design. Not only was the 5-min peak power 19% higher, the average charging power was also found to be 37% higher. The reason lies in the fact that the finned design had a heat transfer surface 9.4 times larger than the non-fined design although the amount of PCM was only 3% larger. On the contrary, the two storage tanks from the University of Lleida used Syltherm 800 as HTF. The finned design finished the charging process 35% earlier than the non-finned design and the average power was 33% higher. In this case the finned design had a heat transfer surface 4.7 times larger than the non-fined design and it had 3% less PCM. However, the 5-min peak power of the finned design was 38% lower. This is due to technical issues in the stabilization of the HTF temperature at the beginning of the charging process with the finned design. As a result, the inlet HTF temperature took longer to achieve the operation temperature and therefore the HTF temperature difference between the inlet and outlet of the tank was kept lower at the beginning.

From the temperature profiles shown in Fig. 9, it can be observed that the non-finned designs created a large spread in the increase of the PCM temperature at different locations throughout the vessel. In addition, the measured PCM temperatures were in general below the HTF outlet temperature during most of the measurement time. This indicates that considerable temperature gradients were present and that the PCM temperature was a very local variable. In the VITO design, the average temperature readings at different positions were all above the HTF outlet temperature after 1 h. These results show that the addition of fins greatly increased the potential to store or gain heat from a large volume of PCM. Both designs from the University of Lleida behaved similarly, with a progressive PCM temperature increase according to its distribution within the storage tanks. The PCM located at the initial sections of the tubes bundle (represented by the temperature sensor $T_{PCM.2}$) showed a faster response than the PCM located at final ones (represented by the temperature sensor $T_{PCM.5}$), as a

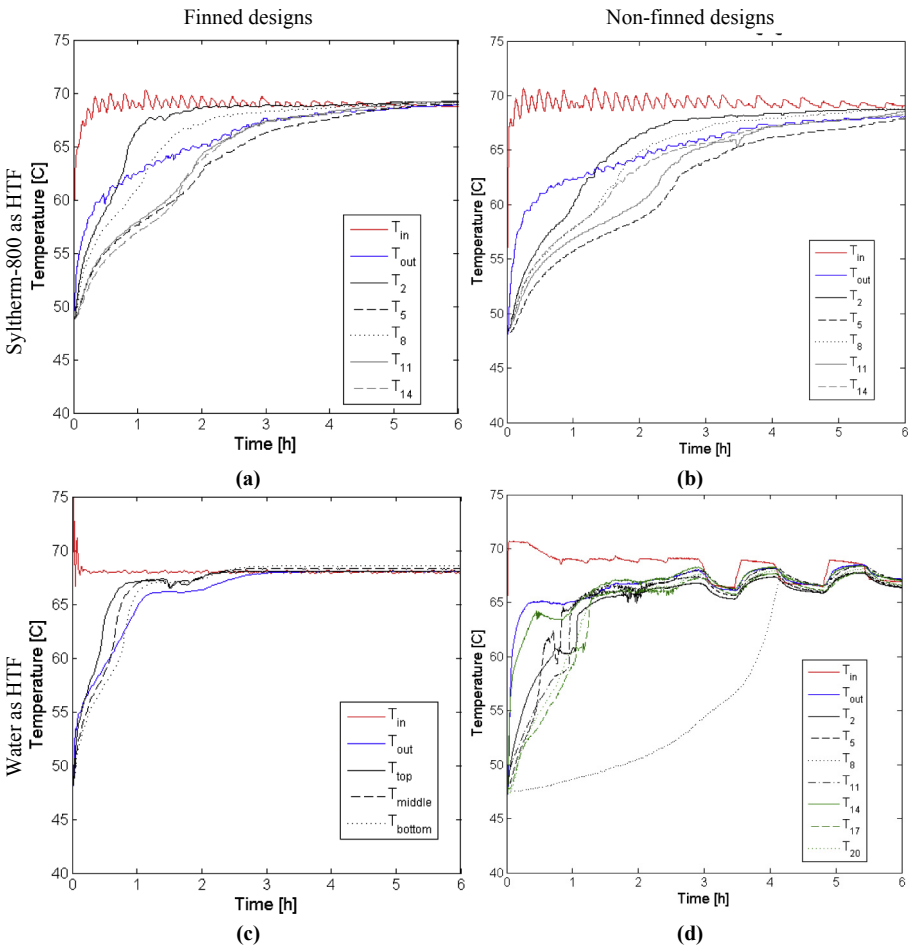

Fig. 9. Temperature profiles during the charging of the inlet and outlet HTF sensors as well as selected PCM sensors shown: (a) University of Lleida (without fins); (b) University of Lleida (with fins); (c) VITO; (d) Glen Dimplex.

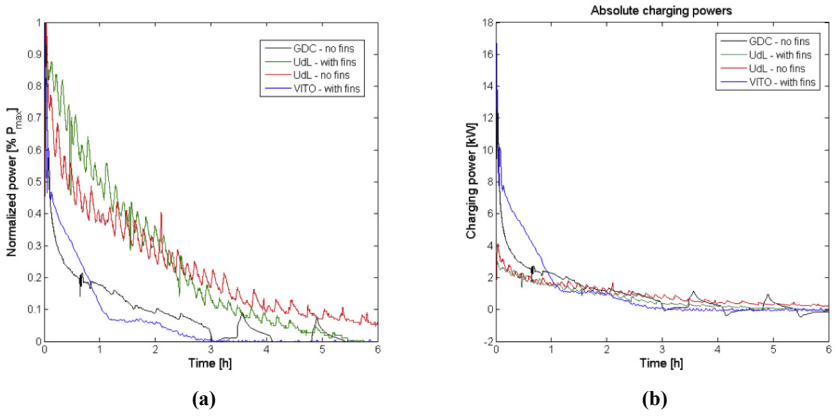

Fig. 10. Experimental power profiles during charging for the different setups: (a) Normalised power profiles. The instantaneous peak power of each design is set to 1 for each case; (b) Absolut power profile.

result of the HTF flow direction. The only difference between both designs was that the finned design had a faster response.

From the power profiles shown in Fig. 10, it can be seen that the finned designs had a high influence on the heat transfer rates at the beginning of the processes, which decreased as the charging processes continued. At the beginning, the increase of the heat transfer surface reduced the thermal resistance of the system, which was dominated by the conduction heat transfer mechanism, since a larger amount of PCM was in direct contact with a surface at a higher temperature. As the PCM started the phase change process however, convection heat transfer dominated and the temperature difference between the heat transfer surface and the PCM progressively reduced. Therefore, the influence of the fins did not become as relevant. Consequently the addition of fins is an

Table 5
Key performance indicators for the different storage designs.

Institution	Energy charged [kWh]	Average power [kW]	5-min peak power [kW]	Peak power -Energy ratio [1/h]	Time [min]
UdL – no fins	5.27	1.42	3.46	0.66	222
UdL – with fins	5.17	1.89	2.51	0.49	164
Glen Dimplex – no fins	6.49	2.04	9.35	1.44	180
VITO – with fins	6.84	2.79	11.09	1.62	145

interesting technique for partial charging and discharging processes.

3.4. Influence of the HTF

The influence of the HTF on the LHTES system thermal performance has been evaluated by comparing the non-finned designs of the University of Lleida and Glen Dimplex because of the similarities on their designs.

As stated earlier, the University of Lleida storage facility used silicone Syltherm 800 as HTF and the Glen Dimplex storage facility used water. Syltherm 800 has considerably different properties with respect to water as observed in Fig. 1. Since both HTF behave under the laminar flow regime, the two main thermophysical properties involved in the heat transfer were the specific heat and the thermal conductivity. Notice that in both cases water had higher results within the temperature range under which the experimentation was carried out: 3 times larger with the specific heat and 4.9 larger with the thermal conductivity. Hence, for a given flow rate and temperature range, water can absorb, transport and release more thermal energy than Syltherm 800.

The previous statements were experimentally validated with the results obtained. From the temperature profiles shown in Fig. 9 it can be seen that the Glen Dimplex design showed a faster response and finished the charging process earlier (decrease of 23% in the charging process time) than the University of Lleida design although its storage system contained 10% more PCM. Moreover, from the power profiles shown in Fig. 10, it can be seen that during the first hour the Glen Dimplex design showed much higher results, with the 5-min peak power being 2.7 times higher than the University of Lleida design. This result shows that the higher the temperature difference between the HTF and the PCM, the higher the influence of the HTF on the heat transfer. After the first hour of the process, both designs showed the same behaviour since the temperature difference decreased and convection from the PCM dominated as the heat transfer type. At the end of the process, the average power transferred by the water was 44% higher than the power transferred by Syltherm 800.

4. Conclusions

In this paper four LHTES systems, using two different design philosophies (finned and non-finned tubes) and two different HTF (water and silicone Syltherm-800), have been experimentally tested and compared.

Paraffin RT 58 was selected as PCM. Different charging processes within the temperature range of 48–68 °C and at a HTF mass flow rate of 500 kg/h were tested. A DSC analysis was carried out with samples of the PCM used by the three institutions. Results showed slight differences between the results of the samples caused by the inherent DSC errors, the mass of the samples and their technical grade. Therefore, these results allowed the three institutions to perform a good comparison.

From an experimental point of view, it has been shown that the use of finned heat exchangers, in combination with water as HTF, provided the most optimal results for a set of KPIs defined in this paper, both for short-term (peak power) and long-term (average power and charge time) purposes. For the same heat transfer fluid, results showed that finned designs (4.7–9.4 times more heat transfer surface) showed results up to 40% better. On the contrary, for the same design, water (which has a specific heat 4.9 times larger and a thermal conductivity 3 times larger than silicone Syltherm 800), showed results up to 44% higher.

Acknowledgments

The research leading to these results has received funding from the European Commission Seventh Framework Programme (FP/2007–2013) under grant agreement No ENER/FP7/295983 (MERITS) and under Grant agreement N°PIRSES-GA-2013-610692 (INNOSTORAGE), and from the European Union's Horizon 2020 research and innovation programme under grant agreement No 657466 (INPATH-TES). The work is partially funded by the Spanish government (ENE2015-64117-C5-1-R (MINECO/FEDER) and ULLE10-4E-1305). The authors would like to thank the Catalan Government for the quality accreditation given to the research group GREA (2014 SGR 123). Jaume Gasia would like to thank the Departament d'Universitats, Recerca i Societat de la Informació de la Generalitat de Catalunya for his research fellowship (2017FI_B 00092).

References

[1] H. Mehling, L.F. Cabeza, Heat and Cold Storage with PCM. An up to Date Introduction into Basics and Applications, Springer-Verlag, Berlin, Germany, 2008. ISBN: 979-3-540-68556-2.
[2] B. Zalba, Marın José Ma, L.F. Cabeza, H. Mehling, Review on thermal energy storage with phase change: materials, heat transfer analysis and applications, Appl. Therm. Eng. 23 (2003) 251–283, http://dx.doi.org/10.1016/s1359-4311(02)00192-8.
[3] F. Agyenim, N. Hewitt, P. Eames, M. Smyth, A review of materials, heat transfer and phase change problem formulation for latent heat thermal energy storage systems (LHTESS), Renew. Sustain. Energy Rev. 14 (2010) 615–628, http://dx.doi.org/10.1016/j.rser.2009.10.015.
[4] A. Trp, K. Lenic, B. Frankovic, Analysis of the influence of operating conditions and geometric parameters on heat transfer in water-paraffin shell-and-tube latent thermal energy storage unit, Appl. Therm. Eng. 26 (2006) 1830–1839, http://dx.doi.org/10.1016/j.applthermaleng.2006.02.004.
[5] H.A. Adine, H.E. Qarnia, Numerical analysis of the thermal behaviour of a shell-and-tube heat storage unit using phase change materials, Appl. Math. Model. 33 (2009) 2132–2144, http://dx.doi.org/10.1016/j.apm.2008.0.
[6] W.-W. Wang, K. Zhang, L.-B. Wang, Y.-L. He, Numerical study of the heat charging and discharging characteristics of a shell-and-tube phase change heat storage unit, Appl. Therm. Eng. 58 (2013) 542–553, http://dx.doi.org/10.1016/j.applthermaleng.2013.04.063.
[7] M. Bechiri, K. Mansouri, Analytical solution of heat transfer in a shell-and-tube latent thermal energy storage system, Renew. Energy 74 (2015) 825–838, http://dx.doi.org/10.1016/j.renene.2014.09.010.
[8] M. Akgün, O. Aydın, K. Kaygusuz, Experimental study on melting/solidification characteristics of a paraffin as PCM, Energy Convers. Manag. 48 (2007) 669–678, http://dx.doi.org/10.1016/j.enconman.2006.05.014.
[9] M. Medrano, M. Yilmaz, M. Nogués, I. Martorell, J. Roca, L.F. Cabeza, Experimental evaluation of commercial heat exchangers for use as PCM thermal storage systems, Appl. Energy 86 (2009) 2047–2055, http://dx.doi.org/10.1016/j.apenergy.2009.01.014.
[10] K.A. Ismail, M.M. Abugderah, Performance of a thermal storage system of the vertical tube type, Energy Convers. Manag. 41 (2000) 1165–1190, http://

dx.doi.org/10.1016/s0196-8904(99)00140-5.
[11] R. Hendra, H.T. Mahlia, H. Masjuki, Thermal and melting heat transfer characteristics in a latent heat storage system using mikro, Appl. Therm. Eng. 25 (2005) 1503–1515, http://dx.doi.org/10.1016/j.applthermaleng.2004.09.009.
[12] F. Agyenim, P. Eames, M. Smyth, Heat transfer enhancement in medium temperature thermal energy storage system using a multitube heat transfer array, Renew. Energy 35 (2010) 198–207, http://dx.doi.org/10.1016/j.renene.2009.03.010.
[13] M.K. Rathod, J. Banerjee, Thermal performance enhancement of shell and tube Latent Heat Storage Unit using longitudinal fins, Appl. Therm. Eng. 75 (2015) 1084–1092, http://dx.doi.org/10.1016/j.applthermaleng.2014.10.074.
[14] R.V. Seeniraj, R. Velraj, N.L. Narasimhan, Thermal analysis of a finned-tube LHTS module for a solar dynamic power system, Heat Mass Transf. 38 (2002) 409–417, http://dx.doi.org/10.1007/s002310100268.
[15] S. Hosseinizadeh, F. Tan, S. Moosania, Experimental and numerical studies on performance of PCM-based heat sink with different configurations of internal fins, Appl. Therm. Eng. 31 (2011) 3827–3838, http://dx.doi.org/10.1016/j.applthermaleng.2011.07.031.
[16] A. Gil, E. Oró, L. Miró, G. Peiró, Á. Ruiz, J.M. Salmerón, et al., Experimental analysis of hydroquinone used as phase change material (PCM) to be applied in solar cooling refrigeration, Int. J. Refrig. 39 (2014) 95–103, http://dx.doi.org/10.1016/j.ijrefrig.2013.05.013.
[17] J. Gasia, L. Miró, A.D. Gracia, C. Barreneche, L. Cabeza, Experimental evaluation of a paraffin as phase change material for thermal energy storage in laboratory equipment and in a shell-and-tube heat exchanger, Appl. Sci. 6 (2016) 112, http://dx.doi.org/10.3390/app6040112.
[18] RT58 data sheet. Available online: http://www.rubitherm.de/english/download/Techdata_%20RT58_EN.PDF. Last Accessed 6 February 2016.
[19] Syltherm 800 product information. Available online: http://www.loikitsdistribution.com/files/syltherm-800-technical-data-sheet.pdf. Last Accessed 5 August 2016.